

## Dynamical evolution of the surface microrelief under multiple-pulse-laser irradiation: An analysis based on surface-scattered waves

A. Barborica

*Physics Department, University of Bucharest, P.O. Box MG-11, Magurele, RO-76900 Bucharest, Romania*

I. N. Mihailescu

*Laser Department, Institute of Atomic Physics, P.O. Box MG-54, Magurele, RO-76900 Bucharest, Romania*

V. S. Teodorescu

*Institute of Physics and Technology of Materials, P.O. Box MG-7, Magurele, RO-76900 Bucharest, Romania*

(Received 11 March 1993; revised manuscript received 15 November 1993)

We introduce a theoretical analysis of the temporal and spatial evolution of the surface topography of solids following interference between incident and scattered pulsed laser beams. The essential role played by the nonlinear delayed feedback in the laser-radiation-surface system is considered. We show that it finally determines the surface topography evolution from pulse to pulse. In order to complete the analysis, numerical calculations have been conducted under the hypothesis of strong attenuation of laser radiation into the sample and of a limited heat diffusion during the action of a laser pulse. We predict an evolution from very simple to complex (chaotic) structures under multiple-pulse-laser irradiation of solid surfaces. This evolution is determined by some key irradiation parameters: initial surface microrelief, incident laser intensity, and the number of applied laser pulses. Experiments were performed in order to check the main predictions of the theoretical analysis. The system of transversal excited atmospheric pressure-CO<sub>2</sub> laser radiation ( $\lambda=10.6\ \mu\text{m}$ )—interacting with fused silica was chosen as appropriate for performing test experiments. Optical microscopy studies of laser-treated zones evidenced special modifications of the surface topography in good accordance with the conclusions following from the theoretical analysis. The theoretical analysis is also in good agreement with some available data from the literature, at the same time providing a coherent interpretation of previously unexplained behaviors.

### I. INTRODUCTION

The formation of surface structures under pulsed laser irradiation has been observed in a large variety of materials, such as lead, copper, bronze, steel, and so on, differing very much from one another in terms of thermo-physical properties. Moreover, the surface structures are formed under the action of laser radiation whose wavelength ranges from uv to far ir. There is an extensive literature dedicated to this subject,<sup>1-12</sup> but none of the previously developed models (e.g., Refs. 1-4) give a satisfactory explanation for the formation of all surface structures for observed or the evolution from ordered to disordered structures.<sup>5,6</sup> This is why we are proposing a different approach, which considers the formation of surface structure of any complexity as a consequence of the evolution of a nonlinear dynamic system with delayed feedback.

Experimentally observed surface structures exhibit an evolution from order to disorder, as a control parameter like the intensity of the laser radiation varies.<sup>5,6</sup> The route from order to disorder up to the onset of chaos passes through the development of high-order surface structure, showing a simultaneous modulation with several wavelengths,<sup>6-8</sup> and seems to be the one commonly known in the literature as the Feigenbaum (or subharmonic) route to chaos.<sup>13</sup> Our approach is based

upon the observation of the similarity between this evolution and that of well-known dynamic systems such as ring cavities,<sup>14</sup> hybrid electro-optical devices,<sup>15,16</sup> laser resonators,<sup>17</sup> and so on. While in most dynamic systems a certain physical quantity exhibits a periodic or chaotic behavior in time, surface structures show a spatial periodicity or chaos. In the case of surface-structure formation, the interaction between the laser radiation and the surface is not completely understood, so one cannot yet establish in a direct way an appropriate model that would account for all the surface structures observed. In spite of that, the main features of the surface structures and their evolution with the appropriate control parameters resemble strikingly those observed in the above-mentioned dynamic systems. That leads us to assume that the scenario may be the same, although the physical phenomena are different.

In a dynamic system, chaos can appear in several ways. For instance, in most systems, a usually complex nonlinear interaction Hamiltonian can lead to chaotic behavior. Instabilities have also been observed in systems whose Hamiltonians lead to stable solutions but where there is a delayed feedback loop. These instabilities, sometimes referred to as Ikeda instabilities,<sup>18,19</sup> have been seen in extensively studied optical ring cavities,<sup>14</sup> hybrid electro-optical devices,<sup>15,16</sup> and lasers with delayed feedback,<sup>20</sup> and are to be expected in other systems with de-

layed feedback as well.

In the next section of this paper we make assumptions which allow us to describe the process of surface-structure formation as the evolution of a dynamic nonlinear system with delayed feedback. Then, the evolution from order to disorder follows in a natural way from the analysis of such a dynamic system. Illustrative results of this analysis are presented and discussed in Sec. III. An experiment, described in Sec. IV, was designed and performed in order to check some predictions of the theoretical and numerical analysis.

## II. THE MODEL

### A. Main assumptions

In the large amount of literature dedicated to this subject, it is generally accepted that surface-structure formation usually involves two major steps: a nonuniform deposition of energy and a mechanism, generally a thermal one, that converts the absorbed energy into a surface deformation.

One of the mechanisms leading to nonuniform deposition of energy is the interference between the surface-scattered wave (SSW) and the incident laser wave.<sup>3,9</sup> We demonstrate that even such a simple mechanism can explain the development of ordered and, what is more important, of disordered surface structures, under appropriate conditions. The SSW mechanism requires the presence of an initial microrelief, roughness, or surface defect acting as a scattering center.<sup>2,3,9</sup> It is this last case we particularly consider in our analysis.

The mechanism that converts the locally absorbed energy into a surface deformation (via a thermal or electrostrictive process) is a complex one and to discuss it here is beside the point. For the purpose of our demonstration, we will make the approximation of a simple linear dependence of the surface deformation on the local value of the absorbed energy. As we have checked, such a linear approximation does not alter significantly the qualitative evolution of the analyzed dynamic system, which is in turn strongly influenced by the presence of a delayed feedback loop. Moreover, even with this simple approximation, the whole system remains strongly nonlinear, since the feedback loop involves scattering of light, interference, and squaring of the resulting electric field in order to obtain the locally absorbed energy.

We assume the following scenario leading to surface-structure formation: the nonuniform deposition of energy during the action of the laser pulse leads to a delayed surface modification. The feedback loop closes with the next laser pulse, when the scattering of light takes place over the previously modified surface. As we have mentioned, the resulting distribution of energy over the surface is in a nonlinear relation with its shape. In conclusion, the surface shape at the beginning of a certain pulse will be a *delayed nonlinear function* of the surface shape at the beginning of the previous pulse.

According to this scenario, one is entitled to adopt the following hypothesis establishing a direct correspondence between the process of surface-structures development and other dynamic systems with delayed feedback: the

intrapulse feedback effects<sup>6</sup> are to be neglected as compared to the interpulse feedback effects. The presence of the intrapulse feedback makes calculation of the scattered and resulting field very difficult, since the surface is continuously changing under the action of the resulting field itself. One can neglect the intrapulse feedback effects in two cases:

(i) The scattering of light by the initial defect is much more important than the scattering by the developing surface structure. This case corresponds to intensities of laser radiation low enough to enable the development, during the laser pulse, of small-amplitude surface structures only, with a less significant contribution to scattering than the initial defect. This generally applies to the formation of so-called resonant surface structures. In detail, this problem will be considered again in Sec. III of this paper. These resonant surface structures have simple geometrical characteristics and a single wavelength  $\Lambda$  in a direct, simple, relation with the parameters of the incident laser radiation. The wavelength  $\Lambda$  of a resonant surface structure forming as a consequence of the action of laser radiation of wavelength  $\lambda$ , linearly polarized in the plane of incidence, and falling onto the surface at an incidence angle  $\alpha$ , is given<sup>3,9</sup> by the relation:

$$\Lambda = \frac{\lambda}{1 \pm \sin \alpha} . \quad (1)$$

We shall refer hereafter to  $\Lambda$  given by (1) as the fundamental wavelength and to the corresponding wave vector  $g = 2\pi/\Lambda$  as the fundamental wave vector.

(ii) The laser pulse duration is small compared to the characteristic duration of structures formation on the surface submitted to laser irradiation. Then, the surface does not undergo major changes during the laser pulse, but only after its end. This corresponds to experimental evidence of the formation of surface structures known in the literature as "nonresonant." These surface structures, which do not have geometrical characteristics in direct relation with the parameters of the incident laser radiation, arise during the cooling stage subsequent to pulsed laser irradiation.<sup>3,4</sup> As a matter of fact, this amounts to considering the laser pulse ultimately as a Dirac function, so that the convolution integral, very difficult to calculate, between the pulse shape and the surface modification is reduced to a single value.

We emphasize that the surface undergoes significant changes during the cooling stage. This means that there is a delay between the nonuniform deposition of energy and the settling of the surface shape into its final form. The presence of this delay is essential for our dynamical analysis.

### B. Basic equations

We calculate the electric field resulting from the scattering of light by the whole irradiated surface with an approximate diffraction integral that best suits the bidimensional geometry we have chosen. Such an approach is justified by the following two considerations: there is no exact analytic solution available of the Maxwell equa-

tions for an arbitrary surface profile, and as will be further shown, by numerically solving our equations we get the same results as authors who have solved the Maxwell equations, in some particular cases.<sup>2,3</sup> Moreover, numerical solution of two-dimensional (2D) Maxwell equations would require a large amount of calculation, while the method we are presenting here requires only a 1D numerical integration along the surface contour.

We use a method which is derived from the Huyghens-Fresnel principle.<sup>21</sup> Thus we decompose the laser-irradiated surface into small domains which we consider as semi-infinite apertures (see Fig. 1) which are a source of secondary, reflected waves. For a width of an arbitrary aperture, denoted by  $m$ , much smaller than the incident laser wavelength, the angular distribution of the intensity is constant.<sup>21</sup> The scattered waves having cylindrical symmetry, the intensity at a point  $P$  placed at a distance  $|\mathbf{r}-\mathbf{r}_m|$  from the aperture much larger than its width  $w$ , is given by:

$$I_{0m} = I_0 \frac{w}{\pi |\mathbf{r}-\mathbf{r}_m|}, \quad (2)$$

where  $\mathbf{r}$  and  $\mathbf{r}_m$  are the position vectors of the aperture  $m$  and the point  $P$ , and  $I_{0m}$  is the intensity of the radiation emerging from the aperture  $m$ , as a function of the incident laser intensity  $I_0$  and the aperture's tilt to the direction of propagation of the laser radiation, that is:

$$I_{0m} = I_0 R(\alpha + \varphi) \cos(\alpha + \varphi). \quad (3)$$

In Eq. (3), we have denoted by  $\alpha$  the incidence angle of the laser radiation against the plane surface, and by  $\varphi$  the slope of the surface,  $\alpha + \varphi$  being thus the local incidence angle of the radiation on the surface (see Fig. 1). The reflectivity  $R(\alpha + \varphi)$  of the surface depends on the local incidence angle and the polarization state of the incident wave, according to the Fresnel relations.<sup>3,21,22</sup> For the purpose of our simulations, we have chosen the incident wave to be polarized in the plane of incidence.

Taking into account that  $I_0 \sim E_0^2$  (with  $E_0$  the magnitude of the electric field in the incident beam), we obtain from Eqs. (2), (3) the following relation for the electric field  $E_m$  at a distance  $|\mathbf{r}-\mathbf{r}_m| \geq w$  from the aperture  $m$ :

$$E_m(\mathbf{r}) = E_0 R^{1/2}(\alpha + \varphi) \cos^{1/2}(\alpha + \varphi) \left( \frac{w}{\pi} \right)^{1/2} |\mathbf{r}-\mathbf{r}_m|^{-1/2}. \quad (4)$$

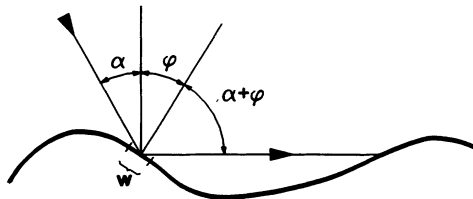


FIG. 1. Detail of the irradiated surface, illustrating the scattering of light on the surface. We have denoted by  $\alpha$  the incidence angle of the laser radiation, by  $\varphi$  the tilting of the scattering surface, and by  $w$  the width of the aperture we take into account.

The waves produced by all the apertures are considered to interfere with one another and with the incident laser wave, producing a certain intensity distribution over the surface. The relation which gives the vector value  $\mathbf{E}$  of the field at a certain point of the surface follows immediately from Eqs. (2)–(4), taking into account the phases of every interfering wave:

$$\mathbf{E}(\mathbf{r}) = \mathbf{E}_0 e^{i\mathbf{k}_0 \cdot \mathbf{r}} - \sum_m \mathbf{E}_{m(\mathbf{r})} e^{i\mathbf{k}_0 \cdot \mathbf{r}} e^{i\mathbf{k}_m \cdot (\mathbf{r}-\mathbf{r}_m)}, \quad (5)$$

where  $\mathbf{k}_0$  and  $\mathbf{k}_m$  are the wave vectors of the incident and the scattered waves, respectively, having equal modulus ( $k_m = k_0 = 2\pi/\lambda$ ) but different orientations. The minus in front of the sum over all the apertures is a consequence of the change of phase at the reflection on the surface. In calculating the sum in (5) we have assumed that the surface structures are not deep, i.e., the amplitude of the surface structure is much smaller than its wavelength, so one can neglect multiple scattering.

The resulting intensity  $I(\mathbf{r})$  of the radiation at the point  $P(\mathbf{r})$  is proportional to the square of the corresponding electric field ( $I(\mathbf{r}) \sim E(\mathbf{r})^2$ ). Only a part of it ( $I_a$ ) is absorbed, depending on the local absorptivity  $A(\chi)$ , where  $\chi$  is the angle between the wave vector of the resulting field  $\mathbf{E}(\mathbf{r})$  and the normal to the surface at the given point  $P$ ,

$$I_a(\mathbf{r}) \sim A(\chi) E(\mathbf{r})^2. \quad (6)$$

The local value of the absorptivity results from the above-mentioned Fresnel relations, taking into account the fact that the polarization of both the incident and scattered fields is in the plane of incidence.

The absorbed radiation usually leads to a local rise in temperature. As mentioned in the previous section, we are assuming that the temperature rise follows the locally absorbed energy in a linear way:

$$\Delta T(\mathbf{r}) \sim I_a(\mathbf{r}). \quad (7)$$

This assumption is valid only under the hypothesis that the heat does not diffuse significantly into the irradiated sample during the laser pulse duration. In other words, the heat diffusion length  $L_T$  into the irradiated material during the laser pulse duration  $\tau$  should be much shorter than the wavelength  $\Lambda$  of the surface structure:

$$L_T \ll \Lambda. \quad (8)$$

In Eq. (8),  $L_T = \sqrt{k\tau}$  ( $k$  is the thermal diffusivity of the sample) and  $\Lambda$  is given by Eq. (1). For a given material, one can find from Eq. (8) the relation that must obey the laser pulse duration in order to ensure that Eq. (7) is valid:

$$\tau \ll \frac{\Lambda^2}{k}. \quad (9)$$

Usually the delay between two successive pulses is several orders of magnitude greater than the laser pulse duration, so the heat diffusion cannot be neglected during the time elapsed between two pulses. For the sake of simplicity, we have assumed an exponential decay of the surface temperature, close to the real decay of the temperature

described by more complicated relations.<sup>22–24</sup>

The local rise in temperature will cause a deformation of the surface through thermal expansion, local melting, temperature dependence of the surface tension, and so on. For our demonstration it is enough to assume that whatever process takes place, it causes a local deformation of the surface. Even a simple linear process which converts the local temperature into a surface deformation [ $\Delta h(\mathbf{r}) \sim \Delta T(\mathbf{r})$ ] will not lead to a qualitative change in the results of our analysis since there is a strongly nonlinear process that closes the feedback loop. More pre-

cisely, the nonuniform deposition of energy is not linearly dependent on the surface shape at a certain time, as one can see from Eqs. (2)–(6). Thus we assume that the surface deformation  $\Delta h(\mathbf{r})$  obeys the relation:

$$\Delta h(\mathbf{r}) \sim I_a(\mathbf{r}). \quad (10)$$

Under the assumptions we have made, from (4), (5), (6), and (10), one obtains the deformation of the surface at the end of the relaxation (cooling) process subsequent to a certain laser pulse, i.e., at the beginning of the next laser pulse:

$$\Delta h(\mathbf{r}) = \text{const} \times A(\chi) \left| \mathbf{E}_0 e^{i\mathbf{k}_0 \cdot \mathbf{r}} - E_0 \sum_m R^{1/2}(\alpha + \varphi) \cos^{1/2}(\alpha + \varphi) \left( \frac{w}{\pi} \right)^{1/2} e^{i\mathbf{k}_0 \cdot \mathbf{r}_m} e^{i\mathbf{k}_m \cdot (\mathbf{r} - \mathbf{r}_m)} |\mathbf{r} - \mathbf{r}_m|^{-3/2} (\mathbf{r} - \mathbf{r}_m) \right|^2. \quad (11)$$

It is to be noticed that the surface shape over which the sum in Eq. (11) runs is the one obtained before the applied laser pulse. Also, the apertures into which we have decomposed the surface, having improper orientations (the emerging waves do not reach the point  $P$  at which we calculate the surface deformation), do not make any contribution to the sum in Eq. (11). The constant factor on the right-hand side of Eq. (11) may take values differing from one another by several orders of magnitude, depending on the particular phenomena leading to the deformation of the surface, and on the optical, mechanical, and thermal properties of the irradiated material. That is why we do not give its explicit form, which would inevitably be a very particular one.

We further obtain for the surface profile at a certain time  $h(\mathbf{r}, t)$ , after its having been submitted to a laser pulse in the form of a nonlinear function of its shape after the previous pulse:

$$h(\mathbf{r}, t) = f[h(\mathbf{r}, t - t_d)] \quad (12)$$

where  $t_d$  is the time elapsed between two subsequent pulses. Relations of this kind characterize many dynamic systems exhibiting bistability and evolution from order to disorder. Thus one expects our particular system to exhibit features resembling those of other dynamic systems.<sup>14–19</sup>

### III. NUMERICAL ANALYSIS

We have performed numerical calculations according to the model introduced above. We have assumed different initial scattering centers, different incidence angles, and various values of the control parameter, which is the intensity of the laser radiation. We observe the evolution of the surface microrelief under the cumulative action of several subsequent laser pulses applied to the same irradiation location. As the aim of this paper is to describe the dynamics of the surface topography, we chose an appropriate set of variables. Instead of the time dependence of the analyzed quantities, we study their dependence on a normalized current coordinate  $x/\lambda$  along a direction in the plane surface. The time is treated as a parameter only, and is taken into account through the number of applied laser pulses. Correspondingly, we

have chosen as conjugate variables the spatial derivatives  $\partial z/\partial x$  of the surface microrelief height as a function of the normalized microrelief height  $z/\lambda$ . This set of variables and parameters has also the advantage of experimental relevance.

For the first set of simulations, we chose a Gaussian shape for the initial scattering center, represented in Fig. 2. The laser radiation linearly polarized in the incidence plane falls on the surface at an incidence angle of  $\alpha = 30^\circ$ .

We note that any modification of the surface microrelief is possible if a characteristic “recording” intensity value is surpassed. In practice,  $I_r$  is the minimum incident intensity that causes an irreversible deformation of the surface microrelief (by melting, plastic deformation, etc.). If  $I_0 < I_r$ , one cannot observe any modification of the surface microrelief. For  $I_0 > I_r$ , the surface changes in accordance with the resulting interference pattern. For this reason, our analysis will be further conducted in terms of the difference  $I_0 - I_r$  between the laser intensity and the specific recording value.

We have used a normalized value of the control parameter  $I_n$ , defined as the ratio between the actual laser intensity  $I_0 - I_r$  and another characteristic threshold value,  $I_{th} - I_r$ . For  $I_0 \leq I_{th}$ , surface structures with a single wavelength given by (1) and a sine-type profile form on the surface as an effect of multiple-pulse irradiation. Accordingly, everywhere in what follows,  $I_n$  stands for

$$I_n = \frac{I_0 - I_r}{I_{th} - I_r}. \quad (13)$$

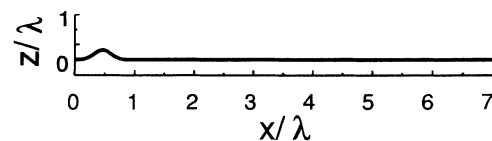


FIG. 2. Surface shape with a Gaussian scattering center. The normalized microrelief height  $z/\lambda$  is represented as a function of the normalized current coordinate  $x/\lambda$  along a direction in the plane surface, where  $\lambda$  is the laser wavelength.

By varying the control parameter  $I_n$ , one can see several effects. For  $I_n=1$  the results of our calculations indicate the formation of single-wavelength surface structures of sine-type shape, as can be seen from Figs. 3(a)–3(c) which represent the shape of the surface within the irradiation spot after the first, fifth, and tenth pulses, respectively. One observation is that the surface structures are stable against the number of subsequent pulses. This stable behavior is maintained even when the number of subsequent laser pulses is increased to tens or even hundreds. The results of our calculations for various incidence angles indicate a perfect accordance between the observed wavelength of the periodical surface structure and that predicted by Eq. (1)—see Figs. 3(a)–3(c). The phase-space diagram in Fig. 4 of the surface after the first pulse shows a simple spiral which converges to the origin, this particular point being the attractor for the phase-space evolution. The attractor at the origin corresponds to quenching of the surface undulations far from the scattering center. The absence of multiple looping in the spiral in Fig. 4 indicates a single spatial frequency with decreasing amplitude.

A different evolution is predicted for  $I_n=10$ . Thus, as one observes from Fig. 5(a), after the first pulse, surface structures are single wavelength and sine type. The second and third pulses induce a further change in morphology [Fig. 5(b)]. A supplementary modulation of the surface with a period of  $3\lambda$  is observed, which is slightly accentuated by the subsequent pulses [Fig. 5(c)]. As we have checked, this structure remains stable after hundreds of subsequent laser pulses.

As we further increase the intensity to  $I_n=100$ , Figs. 6(a)–6(c) show a modulation of the surface with both harmonics and subharmonics of the fundamental wave vector  $g$ . Indeed, the phase-space diagram in Fig. 7 of the surface in Fig. 6(b) confirms by its multiple loops the presence of several spatial frequencies in the surface undulations. Both the frequency and the amplitude of the spatial harmonics can be seen in the Fourier spectrum in Fig. 8 of the surface in Fig. 6(c).

At very high intensity levels,  $I_n=2500$ , the complexity of the surface increases for each pulse [see Figs. 9(a)–9(c)] up to a quasichaotic appearance after three pulses [Fig. 9(c)]. We stress the fact that after the first pulse, the

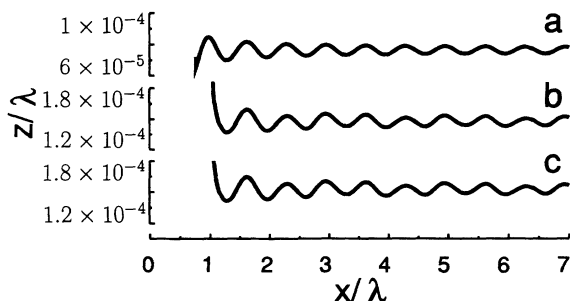


FIG. 3. Surface shape after the (a) first, (b) fifth, and (c) tenth applied laser pulse, for a normalized intensity of  $I_n=1$ . The normalized microrelief height  $z/\lambda$  is represented as a function of the normalized current coordinate  $x/\lambda$  along a direction in the plane surface.

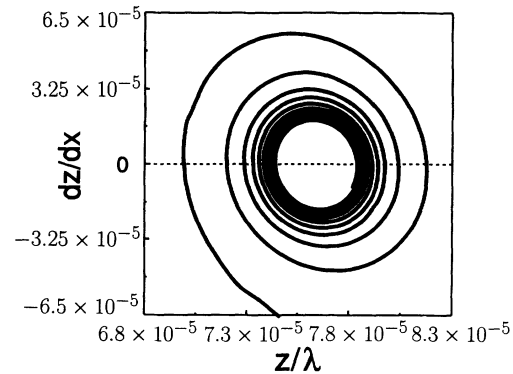


FIG. 4. Phase-space diagram of the surface in Fig. 3(a) (after the first pulse). The spatial derivative  $\partial z/\partial x$  of the surface microrelief height is represented as a function of the normalized current coordinate  $x/\lambda$ .

shape of the surface is of single wavelength sine type again. After the second pulse, besides the fundamental and low-order harmonics and subharmonics of the fundamental, one sees high order spatial harmonics—compare Fig. 10, which is the Fourier spectrum of the surface in Fig. 9(c), to Fig. 8.

In order to elucidate the role of the initial defect in the development of surface structure, we have also chosen two other shapes for the initial scattering center: triangular and hemispherical, shown in Figs. 11(a) and 12(a). Sample results for these particular cases, are presented in Figs. 11(b) and 11(c) and 12(b) and 12(c). The calculations were performed for identical irradiation parameters as in the situations reproduced in Figs. 6(a)–6(c), i.e., linear polarization in the incidence plane,  $I_n=100$ , and  $\alpha=30^\circ$ . One observes no significant qualitative differences between the surface shapes in Figs. 6(a) and 6(b), 11(b) and 11(c), and 12(b) and 12(c). It is therefore apparent that the behavior of the system is mainly determined not by the initial defect, but by the value of the control parameter  $I_n$ .

The most important conclusion following from our analysis is that a practically unlimited variety of surface structures emerge from the relative positions on the intensity scale of the three key intensities characterizing

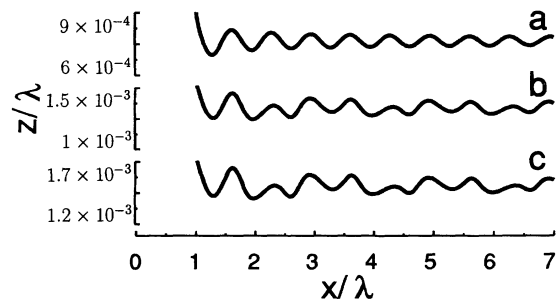


FIG. 5. Surface shape after the (a) first, (b) third, and (c) sixth pulse, for a normalized intensity of  $I_n=10$ . The normalized microrelief height  $z/\lambda$  is represented as a function of the normalized current coordinate  $x/\lambda$  along a direction in the plane surface.

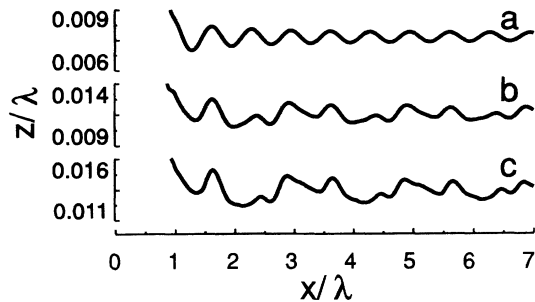


FIG. 6. Surface shape after the (a) first, (b) second, and (c) third pulse, for a normalized intensity of  $I_n = 100$ . The normalized microrelief height  $z/\lambda$  is represented as a function of the normalized current coordinate  $x/\lambda$  along a direction in the plane surface.

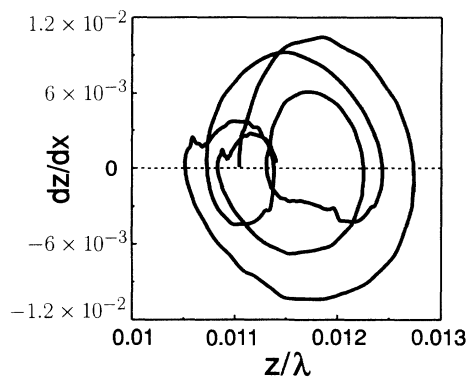


FIG. 7. Phase-space diagram of the surface in Fig. 6(b) (after the second pulse). The spatial derivative  $\partial z/\partial x$  of the surface microrelief height is represented as a function of the normalized current coordinate  $x/\lambda$ .

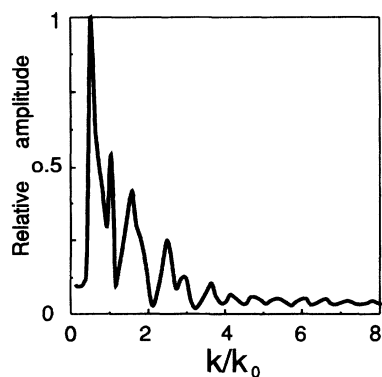


FIG. 8. Fourier spectrum of the surface in Fig. 6(c) (after the third pulse). The relative amplitude of the various spatial frequencies is represented as a function of the normalized grating wave vector  $k/k_0$ , where  $k = 2\pi/x$  and  $k_0 = 2\pi/\lambda$ .

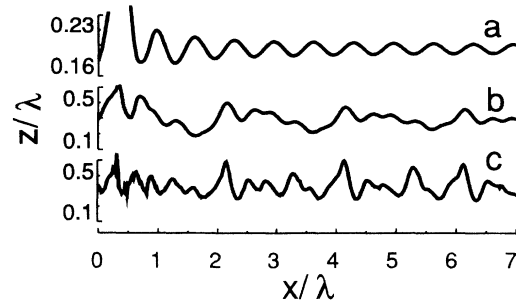


FIG. 9. Surface shape after the (a) first, (b) second, and (c) third pulse, for a normalized intensity of  $I_n = 2500$ . The normalized microrelief height  $z/\lambda$  is represented as a function of the normalized current coordinate  $x/\lambda$  along a direction in the plane surface.

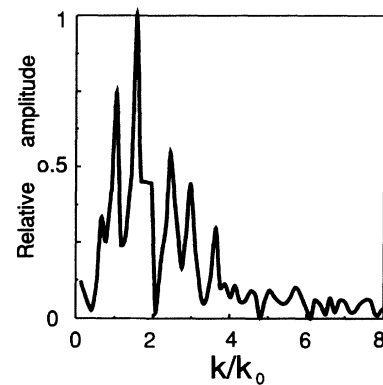


FIG. 10. Fourier spectrum of the surface in Fig. 9(c) (after the third pulse). The relative amplitude of the various spatial frequencies is represented as a function of the normalized grating wave vector  $k/k_0$ , where  $k = 2\pi/x$  and  $k_0 = 2\pi/\lambda$ .

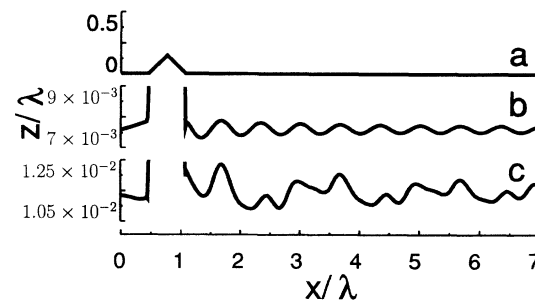


FIG. 11. (a) Surface with a triangular scattering center prior to laser irradiation. Surface shape after (b) the first and (c) the second pulse, for  $I_n = 100$ . The normalized microrelief height  $z/\lambda$  is represented as a function of the normalized current coordinate  $x/\lambda$  along a direction in the plane surface.

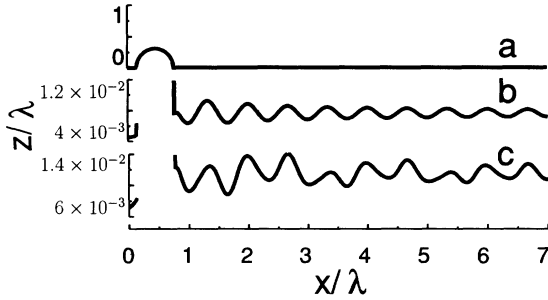


FIG. 12. (a) Surface with a hemispherical scattering center prior to laser irradiation. Surface shape after (b) the first and (c) the second pulse, for  $I_n = 100$ . The normalized microrelief height  $z/\lambda$  is represented as a function of the normalized current coordinate  $x/\lambda$  along a direction in the plane surface.

this process,  $I_r, I_{th}, I_0$ , forming the control parameter  $I_n$  given by Eq. (13). Indeed, if  $I_r$  and  $I_{th}$  are close, relatively small changes of the incident laser intensity  $I_0$  cover the whole range of situations discussed above. Surface shapes differing as much as those observed in Figs. 3–9 are then observed as an effect of a very small increase in the incident laser intensity. On the other hand, the relative positions of the surface melting and ablation thresholds,  $I_m$  and  $I_v$ , compared with the three key intensities of our analysis,  $I_r, I_{th}$ , and  $I_0$ , can lead to the formation of a single type of structure, or even to the absence of surface structures at any incident laser intensity. Indeed if  $I_r < I_v < I_{th}$ , only regular sine-type structures are to be expected when performing a multiple-pulse laser irradiation with an incident intensity  $I_r < I_0 < I_v$ . A further increase in the incident laser intensity above the ablation threshold destroys any surface microrelief by material removal.

In this way, our analysis predicts the formation according to the given experimental conditions of all types of surface structure known from the literature. The common classification of surface structures into resonant and nonresonant structures appears therefore to be obsolete.

Next, it has to be noted that there is a direct, intuitive, interpretation for the observed evolution, based on the interaction between the scattering of the incident beam by the initial defect on the one hand, and by the forming surface structure on the other hand. As one observes from Figs. 3(a), 5(a), 6(a), and 9(a), variation of the control parameter  $I_n$  by three orders of magnitude, results in the same surface shape after the first pulse, a single-wavelength sine-type structure. Moreover, the surface shape after the first pulse is almost the same even for other initial defects, excepting in the vicinity of the defect [see Figs. 11(b) and 12(b)]. The wavelength of the periodical structures is the fundamental one, given by Eq. (1). We think that these observations are a consequence of the fact that after the first pulse the interference pattern is determined only by scattering by the initial defect, with the rest of the surface being not yet rippled. Since the defect has dimensions of the order of magnitude of the incident laser wavelength, one expects that its shape will not considerably affect the interference fringes.

The second pulse always finds a rippled surface having two major characteristics: single-wavelength sine-type ripples on the whole surface, except in the region of the initial defect, and a defect, still present, only slightly deformed by the nonuniform energy absorption. The interference fringes produced by the two scattering factors have to be separately considered. The periodical ripples produce a regular interference pattern which is slightly dephased compared to the ripples. This was also shown in a theoretical study by Guosheng, Fouchet, and Siegmann<sup>2</sup> on the formation of regular periodical surface structures. The initial defect produces a stable interference pattern similar to that obtained after the first pulse. By superimposing these two patterns, one obtains the resulting form of the interference pattern. Depending on the relative contributions of these two factors, we can distinguish two major cases:

(i) *The amplitude of the interference pattern produced by the periodical surface structure can be neglected compared with the amplitude of the pattern produced by the initial scattering center.* This is the case for low incident intensity ( $I_n = 1$ ) in our simulations in Figs. 3(a)–3(c). Then the interference fringes are determined only by scattering by the defect and there are no significant modifications from pulse to pulse, except a certain deepening of the resulting structure when the first pulses are applied, until a stationary state is reached [see Figs. 3(a)–3(c)].

(ii) *The amplitudes of the interference patterns produced by the periodical surface structure and the initial defect are both significant.* Since this resulting pattern is not a simple sum of the two interference patterns, one expects it to be rather complex. The complexity of the resulting surface structure is therefore increased from pulse to pulse. This is the case for high incident laser intensities ( $I_n = 10, 100, 2500$ ) presented in Figs. 5(a)–5(c), 6(a)–6(c), and 9(a)–9(c), respectively. The growing complexity up to a chaotic appearance in Fig. 9(c) takes place through the development of subharmonics and harmonics of the fundamental wave vector  $g$ . This type of evolution is known in the literature as the subharmonic (or Feigenbaum) route to chaos.<sup>13</sup> The onset of chaos is thus explained in a natural way.

#### IV. THE EXPERIMENT

An experiment was designed in order to check some of the predictions of the model and numerical analysis. Special care was taken to choose the correct system of incident laser radiation and substrate. In fact, a basic criterion which has to be fulfilled in order to allow the application of our analysis is that the heat diffusion length during the action of a laser pulse is much smaller than the expected wavelength of the surface structure, i.e.,  $L_T = \sqrt{k\tau} \ll \Lambda$  [see Eqs. (8) and (9)]. We chose therefore the longest available laser wavelength in the mid ir ( $\lambda = 10.6 \mu\text{m}$ ) and fused silica,<sup>12</sup> a material with a rather poor thermal diffusivity ( $\kappa = 7 \times 10^{-7} \text{ m}^2 \text{ s}^{-1}$ ).<sup>23</sup> The transversal excited atmospheric pressure (TEA)-CO<sub>2</sub> laser source was operated in pulses of rather short duration  $\tau_{\text{FWHM}} \geq 150 \text{ ns}$  where FWHM indicates the full width at

half maximum. For this purpose, the laser was fed with an active gas mixture without  $N_2$ . The heat diffusion length  $L_T = \sqrt{k\tau_{FWHM}}$  during a laser pulse duration  $\tau_{FWHM}$  is about  $L_T \approx 0.3 \mu\text{m}$ . Thus, the assumption (8), requiring that the heat diffusion length during a laser pulse should be much less than the fundamental wavelength  $\Lambda$  given by (1), is true at any incidence angle. The radiation was linearly polarized in the plane of incidence. We note that  $CO_2$  laser radiation is strongly attenuated when penetrating into fused silica, a process characterized by a value of the attenuation length which can be as low as  $0.2 \mu\text{m}$ .<sup>23</sup> Accordingly, the laser-radiation penetration depth into the fused silica substrate is negligible compared with the expected surface-structure wavelength. Consequently, as assumed in the model, the interference phenomena inside the bulk are negligible, and the only interference processes to be considered are between the incident laser wave and the scattered wave in the free space above the surface.

We have used samples of fused silica of 30 mm diameter and 3 mm thickness. Before the laser treatment, the samples were optically polished and carefully cleaned. The irradiations were conducted in air. We obtained a large set of irradiation spots on the same sample, corresponding in every case to a different number of subsequent pulses from  $N=1$  to 60 shots, while keeping constant the incident laser fluence and the incidence angle. A series of experiments was performed by varying the incident fluence  $F_0$  in the range  $4\text{--}6 \text{ J cm}^{-2}$ . The repetition rate of the laser pulses was  $\nu \leq 1 \text{ Hz}$ , low enough to ensure a complete relaxation of the laser-induced temper-

ature gradients between two subsequent pulses and a low overall heating of the sample. The irradiated zones were examined by phase-contrast optical microscopy.

The microscopic studies showed surface modifications of the zones subjected to multiple-pulse laser irradiation whenever the incident laser fluence  $F_0$  with every laser pulse exceeds  $4 \text{ J cm}^{-2}$ . This approximately sets the value of the recording fluence  $F_r$  (corresponding to the recording intensity  $I_r$ ) to  $F_r \approx 4 \text{ J cm}^{-2}$ . We note that this value corresponds to the experimentally observed melting threshold of fused silica in the surface layer.<sup>12</sup> Studies of the zones exhibiting morphological transformations after multiple-phase laser treatment support the main predictions of our theoretical model and numerical analysis. Indeed:

(i) The existence was proved of a characteristic threshold value of the incident laser fluence of  $F_{th} \approx 4.1\text{--}4.2 \text{ J cm}^{-2}$ . Below this threshold value, multiple-pulse laser irradiation always results in the formation of a regular sine-type surface structure with a wavelength obeying Eq. (1).

(ii) An interesting evolution is observed when examining the surface structures formed after laser irradiation at higher incident fluences, of  $F_0 \approx 5 \text{ J cm}^{-2}$  [Figs. 13(a)–13(c)]. Thus, as shown in Fig. 13(a), at an incidence angle of  $\alpha = 30^\circ$ , after the action of a few laser shots only, a regular sine-type structure develops with a wavelength of  $\Lambda = \lambda / (1 - \sin 30^\circ) = 7.07 \mu\text{m}$ . One notes the similarity of the structure reproduced in Fig. 13(a) and the surface structures obtained by numerical simulation and given in Figs. 3(a), 5(a), 6(a), and 9(a). When

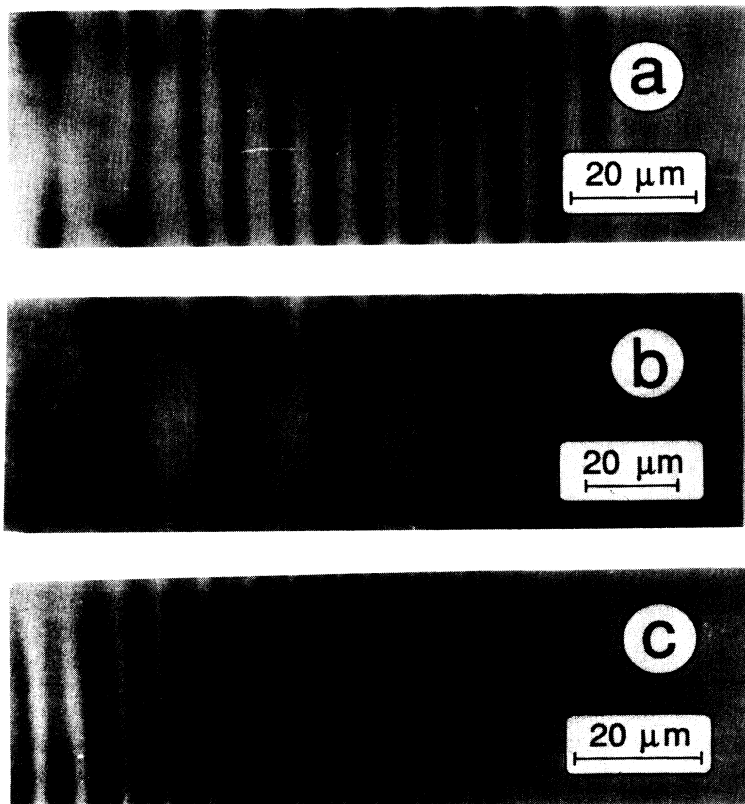


FIG. 13. Optical micrographs of the surface of a fused silica sample submitted to TEA- $CO_2$  laser irradiation ( $\lambda = 10.6 \mu\text{m}$ ,  $\tau_{FWHM} = 150 \text{ ns}$ ,  $\alpha = 30^\circ$ ) after the action of (a) 5, (b) 15, and (c) 60 pulses of  $F_0 \approx 5 \text{ J cm}^{-2}$  incident fluence.



FIG. 14. Optical micrographs of the surface of a fused silica sample submitted to the action of 60 TEA-CO<sub>2</sub> laser pulses ( $\lambda=10.6 \mu\text{m}$ ,  $\tau_{\text{FWHM}}=150 \text{ ns}$ ,  $\alpha=30^\circ$ ) of  $F_0 \approx 6 \text{ J cm}^{-2}$  incident fluence.

multiple-pulse laser treatment of the same location is continued, a supplementary modulation with a period of  $3\Lambda$  is observed [see Fig. 13(b) and compare it to Figs. 5(b), 5(c), and 6(b)]. By increasing the number of applied pulses, sometimes a modulation with a period of a fraction of  $\Lambda$  is observed [Fig. 13(c)].

(iii) Multiple-pulse irradiation with a higher fluence of  $F_0 \approx 6 \text{ J cm}^{-2}$  caused the formation of more complex surface structure presenting a modulation with both harmonics and subharmonics of the fundamental wave vector  $g$  [see Fig. 14 and compare it to Figs. 6(b), 6(c), 9(b), and 9(c)]. A surface structure period of  $2\Lambda$  is observed together with a period much smaller than  $\Lambda$ .

(iv) The observed formation of complex, nonregular surface structures has somehow a random character. We think that this is mainly determined by the random distribution of the initial scattering centers on the surface. This behavior can also be related to the diminishing of both the number and the dimensions of the surface defects by optical polishing and subsequent cleaning of the surface.

The development of several types of surface structure by variation in the incident fluence  $F_0$  from 4.2 to 6  $\text{J cm}^{-2}$ , corresponds to the case discussed in Sec. III when the laser fluences  $F_r$  and  $F_{\text{th}}$  are close, relatively small changes of the incident laser fluence  $F_0$  causing a wide range of surface structures.

## V. DISCUSSION

One has to emphasize that our relatively simple theoretical analysis predicts a large variety of surface-structure types in accordance with the rich existing literature on this subject. Our analysis predicts the formation of single-wavelength sine-type surface structures having simple geometrical characteristics and a wavelength given by Eq. (1). Such surface structures, usually referred to as resonant structures, have been observed in the experiments described in Sec. V [Fig. 13(a)]. This result lends stronger consistency to our analysis, since this particular case is extensively treated in the literature and the predictions of the previously developed models (see, e.g., Ref. 2 and for a review Ref. 3, Chap. V) are practically identical with ours.

The analysis also predicts in a natural way the formation of much more complex surface structures, of the kind visible in Figs. 13(b), 13(c), and 14, whose characteristics could not be related directly to the parameters of the incident laser radiation. On this type of surface structure, usually referred to as nonresonant, the variety of experimental observations is virtually unlimited (for a review see, e.g., Ref. 3, Chap. V).

Moreover, our analysis can explain the formation on the same surface, within the same irradiation spot, of different surface structures, more or less complex, depending on the nature of the initial defect, incidence angle, and local value of the laser intensity.

One of the most interesting behaviors that our analysis predicts is the dependence of the surface-structure profile on the intensity as well as the number of pulses applied onto the same location. We show that for different values of the incident laser intensity, multiple-pulse irradiation can lead not only to a deepening of the forming surface structure—a common case—but also to an evolution from simpler to more complex forms, up to the onset of chaos.

This last result, which to our knowledge has been missing in all previous models, is interesting because it can explain the recently observed phenomenon of laser polishing.<sup>25</sup> At high intensity levels, successive laser pulses onto the same surface induce surface structures which undergo progressive changes in complexity up to the appearance of a macroscopically smooth surface. A simple approach may be derived from this to overcome the drawback caused by ripple formation in some technological processes. In fact, laser treatments, especially in very-large-scale integrated-circuit microelectronics, have often been perturbed, and even compromised, by the omnipresence on the irradiated surface of various types of surface structures hampering the quality of the processed components.<sup>10</sup> We note that from the point of view of our analysis, the phenomenon appears quite natural, and the complete elimination of these behaviors, whenever unwanted can always be achieved by an appropriate choice of the values of the incident laser intensity and the number of applied pulses. At the opposite extreme is the situation when one intentionally induces structures on a surface in order to enhance the energy coupling of the laser radiation to the surface and/or amplify the local values of the electrical field on the surface.<sup>11</sup> Such surface structures can be obtained as an effect of multiple-pulse laser irradiation, according to the predictions of the analysis in this paper. Alternatively, they can be created under the action of capillary acoustical waves in a melted layer as suggested in Ref. 26.

The types of structures that can develop on the surface when the incident laser intensity  $I_0$  is varied are determined by the relative positions on the intensity scale of the key threshold values, introduced in Sec. III:  $I_r$ ,  $I_{\text{th}}$  as well as  $I_m$  and  $I_v$ . Obviously, these threshold values depend on the properties of the irradiated medium and on the parameters of the incident laser radiation.  $I_r$  and  $I_{\text{th}}$  also depend on the particular mechanism leading to surface-structure formation. In some cases the melting

threshold can act as a recording threshold, when the surface structures develop only in the melt, while in other cases surface melting can lead to erasure of the recorded structures. Vaporization always erases surface structures. In the experiment we performed on the system of TEA-CO<sub>2</sub> laser radiation and fused silica, surface melting seems to enable the developing and recording of structures on the surface. The threshold value  $I_{th}$  for the development of complex surface structures is very close to the recording threshold  $I_r$ . Accordingly, relatively small variations of the incident intensity, of about 50%, lead to variations of the normalized intensity, as calculated with Eq. (13), of 1000–2000 %, or even much more, taking into account the uncertainty in determining the threshold values  $I_r$  and  $I_{th}$ . A quite different situation is when one observes in certain laser-radiation–surface systems the formation of only regular surface structures when the incident intensity is varied from  $I_r$  up to the vaporization threshold  $I_v$ . This behavior can also be explained in terms of the relative distribution of the key intensities, when  $I_{th}$  is far away from  $I_r$  and rather close to  $I_v$ .

## VI. CONCLUSIONS

Based on the very abundant experimental and theoretical results reported in the literature on surface structures, we have attempted a direct, intuitive interpretation of these data using the interference between the incident laser wave and surface-scattered waves. The laser-radiation–surface system is treated as a nonlinear dynamic system with delayed feedback. We have considered different shapes of the initial scattering centers present on any surface, and calculated the power cumulatively absorbed by different locations of the surface from one pulse to the next. The effect is the development of a new surface microrelief and an interaction begins between the light scattered by the initial defect and the light scattered by the microrelief formed on the rest of

the surface. In turn, this interaction is determined by such key parameters as the incident laser intensity and the number of applied pulses.

Our analysis naturally points to the possibility of quite different evolutions of the irradiated surface, depending on the values of these parameters. Thus, while the shape of the initial defect seems to make a more or less constant contribution, the surface shape is much more sensitive to the laser incident intensity. One observes that for the same initial situation, an increase of the incident laser intensity may result in two different situations. One is a rather stable situation, when a single-wavelength sine-type surface structure is formed and maintained from the beginning to the end of a prolonged multiple-pulse laser irradiation. An important observation is the similarity of the profile of these surface structures and the well-known profile from many experimental works on resonant surface structures.<sup>11</sup> Conversely, when the laser intensity  $I_0$  exceeds a certain threshold value, the contribution of the surface structures to the interference process becomes significant, and under the cumulative action of a large enough number of pulses, the surface-structure profile grows even more complicated (with either harmonics and/or subharmonics of the fundamental wave vector  $g$ ) till a very intricate appearance, close to chaos, is finally reached.

The analysis predicts in a natural way the evolutions described in the literature. This result is particularly remarkable in view of our initial restriction to the most basic phenomena involved in the interaction process. If account is taken of intrapulse laser effects,<sup>6</sup> or of the specific mechanism leading to a surface deformation, this will not change qualitatively the predictions of this analysis, but will only introduce some quantitative or higher-order corrections. The whole evolution of the process is determined by the relative positions of the incident intensity  $I_0$  and the threshold intensity  $I_{th}$  compared with the intensity  $I_r$  characterizing the recording of structures on the surface.

<sup>1</sup>J. E. Sipe, J. F. Young, J. S. Preston, and H. M. van Driel, *Phys. Rev. B* **27**, 1141 (1983); J. E. Sipe, *J. Opt. Soc. Am. B* **4**, 481 (1987).

<sup>2</sup>Zhou Guosheng, P. M. Fouchet, and A. E. Siegmann, *Phys. Rev. B* **26**, 5366 (1982).

<sup>3</sup>A. M. Prokhorov, V. I. Konov, I. Ursu, and I. N. Mihailescu, *Laser Heating of Metals* (Institute of Physics, Bristol, 1990).

<sup>4</sup>V. M. Emel'yanov, E. M. Zemekov, and V. N. Seminogov, *Kvantovaya Elektron. (Moscow)* **11**, 2283 (1984).

<sup>5</sup>I. Ursu, I. N. Mihailescu, Al. Popa, A. M. Prokhorov, V. P. Ageev, A. A. Gorbunov, and V. I. Konov, *J. Appl. Phys.* **58**, 3909 (1985).

<sup>6</sup>J. E. Sipe and H. M. van Driel, in *Scattering in Volumes and Surfaces*, edited by M. Nieto-Vesperinas and J. C. Dainty (North-Holland, New York, 1990), p. 287.

<sup>7</sup>F. Keilmann and Y. H. Bai, *Appl. Phys. A* **29**, 9 (1982).

<sup>8</sup>P. M. Fauchet and A. E. Siegmann, *Appl. Phys. A* **32**, 135 (1983).

<sup>9</sup>H. M. van Driel, J. E. Sipe, and Jeff F. Young, *Phys. Rev. Lett.*

**49**, 1955 (1982); J. E. Sipe, Jeff F. Young, J. S. Preston, and H. M. van Driel, *Phys. Rev. B* **27**, 1155 (1983); Jeff F. Young, J. S. Preston, H. M. van Driel, and J. E. Sipe, *ibid.* **27**, 1424 (1983); Jeff F. Young, J. E. Sipe, and H. M. van Driel, *ibid.* **30**, 2001 (1984).

<sup>10</sup>A. V. Kuzmichov, V. P. Ageev, and V. I. Konov, in *Proceedings of the International Conference on Laser Microtechnology and Laser Diagnostics of Surfaces—LAMILADIS '91, Chernovtsy, Ukraine, 1991*, edited by N. I. Koroteev and V. Ya. Panchenko, SPIE Proc. Vol. 1723 (SPIE, Bellingham, WA, 1992), p. 21.

<sup>11</sup>I. Ursu, I. N. Mihailescu, A. M. Prokhorov, Al. Popa, V. I. Konov, V. P. Ageev, and V. N. Tokarev, *Appl. Phys. Lett.* **45**, 365 (1984); I. Ursu, I. N. Mihailescu, A. M. Prokhorov, V. I. Konov, and V. N. Tokarev, *J. Appl. Phys.* **61**, 2445 (1987); I. Ursu, I. N. Mihailescu, Calina-Diana Campena, A. M. Prokhorov, V. I. Konov, and V. N. Tokarev, *ibid.* **64**, 6823 (1988).

<sup>12</sup>I. Ursu, I. N. Mihailescu, L. C. Nistor, V. S. Teodorescu, A.

- M. Prokhorov, V. I. Konov, and V. N. Tokarev, *Appl. Opt.* **24**, 3736 (1985).
- <sup>13</sup>J.-P. Eckmann and D. Ruelle, *Rev. Mod. Phys.* **57**, 617 (1985); H. G. Schuster, *Deterministic Chaos. An Introduction*, 2nd ed. (VCH, Weinheim, 1988).
- <sup>14</sup>R. Bonifacio and L. A. Lugiato, *Lett. Nuovo Cimento* **21**, 510 (1978).
- <sup>15</sup>H. M. Gibbs, F. A. Hopf, D. L. Kaplan, and R. L. Shoemaker, *Phys. Rev. Lett.* **46**, 474 (1981).
- <sup>16</sup>M. Okada and K. Takizawa, *IEEE J. Quantum Electron.* **17**, 2135 (1981).
- <sup>17</sup>F. T. Arecchi, R. Meucci, and L. Pezzati, *Phys. Rev. A* **42**, 5791 (1990); in *Proceedings of the European Conference on Optics, Optical Systems and Applications, Rome, 1990*, edited by M. Bertolotti and E. R. Pike, IOP Conf. Proc. No. 115 (Institute of Physics and Physical Society, London, 1991), p. 297.
- <sup>18</sup>K. Ikeda, *Opt. Commun.* **30**, 257 (1979).
- <sup>19</sup>K. Ikeda, H. Daido, and O. Akimoto, *Phys. Rev. Lett.* **45**, 709 (1980).
- <sup>20</sup>F. T. Arecchi, G. Giacomelli, A. Lapucci, and R. Meucci, in *Proceedings of the European Conference on Optics, Optical Systems, and Applications, Rome, 1990* (Ref. 17), p. 285.
- <sup>21</sup>M. Born and E. Wolf, *Principles of Optics*, 6th ed. (Pergamon, New York, 1980).
- <sup>22</sup>W. W. Duley, *CO<sub>2</sub> Lasers, Effects and Applications* (Academic, New York, 1976).
- <sup>23</sup>W. W. Duley, *Laser Processing and Analysis of Materials* (Plenum, New York, 1983).
- <sup>24</sup>M. von Allmen, *Laser-Beam Interactions with Materials*, Springer Series in Materials Science Vol. 2 (Springer-Verlag, Berlin, 1986).
- <sup>25</sup>V. N. Tokarev, A. Yu. Semenov, and V. I. Konov, in *Proceedings of the International Conference on Laser Assisted Materials Processing—LAMP '92, Nagaoka, 1992*, edited by Y. Arata (High-Temperature Society of Japan, Tokyo, 1992), p. 1067; A. Garbunov and V. I. Konov, *ibid.*, p. 1061.
- <sup>26</sup>M. Ganciu, Maria Dinescu, I. N. Mihailescu, and A. Barborica, *Opt. Commun.* **97**, 199 (1993).

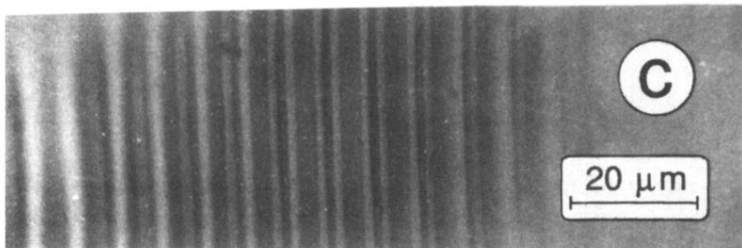
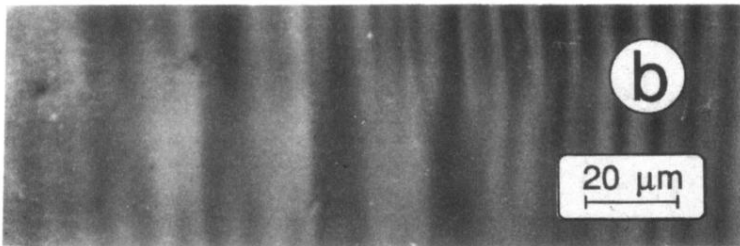
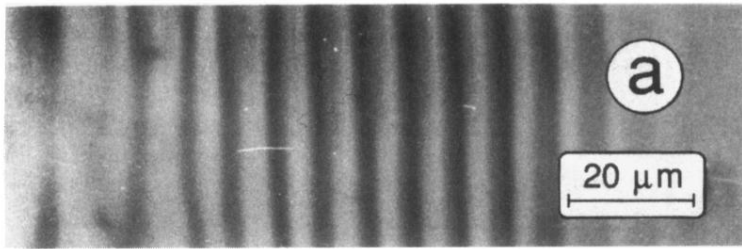


FIG. 13. Optical micrographs of the surface of a fused silica sample submitted to TEA-CO<sub>2</sub> laser irradiation ( $\lambda = 10.6 \mu\text{m}$ ,  $\tau_{\text{FWHM}} = 150 \text{ ns}$ ,  $\alpha = 30^\circ$ ) after the action of (a) 5, (b) 15, and (c) 60 pulses of  $F_0 \approx 5 \text{ J cm}^{-2}$  incident fluence.

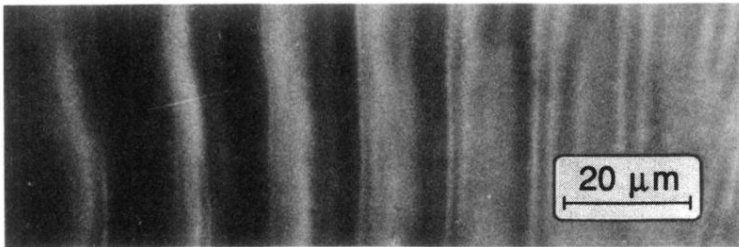


FIG. 14. Optical micrographs of the surface of a fused silica sample submitted to the action of 60 TEA-CO<sub>2</sub> laser pulses ( $\lambda=10.6\ \mu\text{m}$ ,  $\tau_{\text{FWHM}}=150\ \text{ns}$ ,  $\alpha=30^\circ$ ) of  $F_0\approx 6\ \text{J cm}^{-2}$  incident fluence.